AIAA JOURNAL
Vol. 30, No. 5, May 1992

Turbulent Flow Past a Backward-Facing Step: A Critical Evaluation of Two-Equation Models

S. Thangam* and C. G. Speziale†
NASA Langley Research Center, Hampton, Virginia 23665

The ability of two-equation turbulence models to accurately predict separated flows is analyzed from a combined theoretical and computational standpoint. Turbulent flow past a backward-facing step is chosen as a test case in an effort to resolve the various conflicting results that have been published during the past decade concerning the performance of two-equation models. The results obtained demonstrate that errors in the reported predictions of the K-ϵ model have two major origins: 1) numerical problems arising from inadequate resolution, and 2) inaccurate predictions for normal Reynolds stress differences arising from the use of an isotropic eddy viscosity. Inadequacies in near-wall modeling play a substantially smaller role. Detailed calculations are presented that strongly indicate that the standard K-ϵ model—when modified with an independently calibrated anisotropic eddy viscosity—can yield surprisingly good predictions for the back-step problem.

I. Introduction

TURBULENT flow past a backward-facing step has played a central role in benchmarking the performance of turbulence models for separated flows. During the past decade—beginning with the 1980/1981 Stanford conference on complex turbulent flows[1]—various two-equation turbulence models have been tested and compared with the experimental data of Kim et al.[2] and Eaton and Johnston[3] for the back-step problem. Initial results[1] indicated that the standard K-ϵ model, with wall functions, underpredicted the reattachment point by a substantial amount on the order of 20–25%. Several independent studies have been subsequently published using alternative forms of the K-ϵ model, wherein a variety of conflicting results have been resported. For example, Sindir[4] made modifications to account for streamline curvature based on the algebraic stress model of Gibson[5]; some improvements were obtained, although the results were somewhat mixed. Chen[6] performed calculations with a multiple scale K-ϵ model, wherein the turbulent kinetic energy K and the turbulent dissipation rate ϵ were decomposed into low and high wavenumber parts along the lines suggested by Hanjalic et al.[7] Significantly improved results for the reattachment point were obtained (the underprediction was reduced to 5%); however, no detailed comparison of the Reynolds stresses was made. Speziale[8] reported comparable improvements for the back-step problem based on an anisotropic K-ϵ model, which appeared to suggest that the main source of the errors could be due to the use of an isotropic eddy viscosity in the standard K-ϵ model (see also Benocci and Skovgaard[9]). Later, So et al.[10] presented results that seemed to indicate that the right near-wall model could significantly improve the predictions of the K-ϵ model for the back-step problem. Similar claims were made by Karniadakis et al.,[11] who argued that the new near-wall treatment in their K-ϵ model derived by renormalization group (RNG) methods gave rise to drastically improved predictions for the reattachment point. However, Avva et al.[12] presented results which suggested that the large underprediction of the reattachment point attributed to the standard K-ϵ model was due mainly to the fact that the previously reported computations were under-resolved. When sufficient resolution was used, they found that the actual error was only on the order of 10%—a deficiency that they eliminated by introducing an empirical correlation for streamline curvature. Considering the need to accurately predict separated turbulent flows, which can have a wealth of important scientific and engineering applications, it is rather unsettling that such a wide range of conflicting claims still permeate the literature. This establishes the motivation of the present paper, which is to attempt to clarify this issue.

In this paper, the following questions will be addressed:

1) Precisely what does the standard K-ϵ model predict for this back-step problem when the numerics are done properly to insure full resolution of the flowfield and accurate implementation of the boundary conditions?

2) What is the physical source of actual errors in the standard K-ϵ model?

3) Can these errors be eliminated within the framework of two-equation turbulence models without the ad hoc adjustment of constants or the introduction of other arbitrary empiricisms?

These questions will be addressed by conducting sufficiently resolved computations using the standard and anisotropic K-ϵ models, with several independent wall boundary conditions, for the back-step configuration of Kim et al.[2] and Eaton and Johnston.[3] The computations will demonstrate that the standard K-ϵ model yields results within 12% of the experimental data. With the introduction of an anisotropic eddy viscosity, calibrated independently without any ad hoc empiricisms, the K-ϵ model is shown to yield a prediction for the reattachment point that is within a few percent of the experimental result. The physical implications that these results have on the previous work cited will be discussed in detail in the sections to follow.

II. Formulation of the Physical Problem

The problem to be considered is the fully developed turbulent flow of an incompressible viscous fluid past a backward-facing step (a schematic is provided in Fig. 1). Calculations will be conducted for the Kim et al.[2] configuration, wherein the expansion ratio (step height: outlet channel height) E is 1:3

Received May 23, 1991; revision received Aug. 10, 1991; accepted for publication Aug. 13, 1991.

*Visiting Scientist, Institute for Computer Applications in Science and Engineering; Professor, Department of Mechanical Engineering, Stevens Institute of Technology, Hoboken, NJ 07030. Member AIAA.

†Senior Staff Scientist, Institute for Computer Applications in Science and Engineering. Member AIAA.

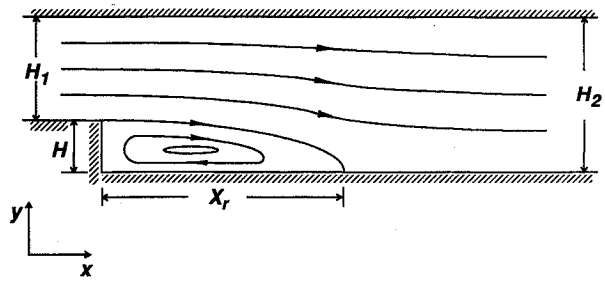

Fig. 1 Physical configuration and coordinate system.

and the Reynolds number $Re = 1.32 \times 10^5$, based on the inlet centerline mean velocity and outlet channel height. The Reynolds averaged Navier-Stokes and continuity equations take the form

$$\frac{\partial \bar{u}}{\partial x} + \frac{\partial \bar{v}}{\partial y} = 0 \tag{1}$$

$$\frac{\partial \bar{u}}{\partial t} + \bar{u}\frac{\partial \bar{u}}{\partial x} + \bar{v}\frac{\partial \bar{u}}{\partial y} = -\frac{\partial \bar{p}}{\partial x} + \nu\left(\frac{\partial^2 \bar{u}}{\partial x^2} + \frac{\partial^2 \bar{u}}{\partial y^2}\right) - \frac{\partial \tau_{xx}}{\partial x} - \frac{\partial \tau_{xy}}{\partial y} \tag{2}$$

$$\frac{\partial \bar{v}}{\partial t} + \bar{u}\frac{\partial \bar{v}}{\partial x} + \bar{v}\frac{\partial \bar{v}}{\partial y} = -\frac{\partial \bar{p}}{\partial y} + \nu\left(\frac{\partial^2 \bar{v}}{\partial x^2} + \frac{\partial^2 \bar{v}}{\partial y^2}\right) - \frac{\partial \tau_{xy}}{\partial x} - \frac{\partial \tau_{yy}}{\partial y} \tag{3}$$

where $\bar{u}$ and $\bar{v}$ are the mean velocity components in the x and y directions, respectively; $\bar{p}$ is the modified mean pressure; τ_{xx}, τ_{xy}, and τ_{yy} are components of the Reynolds stress tensor $\tau_{ij} \equiv \overline{u_i' u_j'}$; and ν is the kinematic viscosity. In the standard K-ϵ model with isotropic eddy viscosity, the Reynolds stress tensor takes the form (see Ref. 13)

$$\tau_{ij} = \frac{2}{3}K\delta_{ij} - 2C_\mu \frac{K^2}{\epsilon}\bar{S}_{ij} \tag{4}$$

where

$$\bar{S}_{ij} = \frac{1}{2}\left(\frac{\partial \bar{u}_i}{\partial x_j} + \frac{\partial \bar{u}_j}{\partial x_i}\right) \tag{5}$$

is the mean rate of strain tensor, $K \equiv \frac{1}{2}\tau_{ii}$ the turbulent kinetic energy, ϵ the turbulent dissipation rate, $\bar{u}_i = (\bar{u}, \bar{v})$ the mean velocity vector, and C_μ a dimensionless constant that is taken to be 0.09. An anisotropic K-ϵ model will be considered—namely, the nonlinear K-ϵ model of Speziale[8]—wherein the Reynolds stress tensor takes the form

$$\tau_{ij} = \frac{2}{3}K\delta_{ij} - 2C_\mu \frac{K^2}{\epsilon}\bar{S}_{ij} - 4C_D C_\mu^2 \frac{K^3}{\epsilon^2} \times \left(\mathring{\bar{S}}_{ij} - \frac{1}{3}\mathring{\bar{S}}_{kk}\delta_{ij} + \bar{S}_{ik}\bar{S}_{kj} - \frac{1}{3}\bar{S}_{kl}\bar{S}_{kl}\delta_{ij}\right) \tag{6}$$

where

$$\mathring{\bar{S}}_{ij} = \frac{\partial \bar{S}_{ij}}{\partial t} + \bar{u}_k\frac{\partial \bar{S}_{ij}}{\partial x_k} - \frac{\partial \bar{u}_i}{\partial x_k}\bar{S}_{kj} - \frac{\partial \bar{u}_j}{\partial x_k}\bar{S}_{ki} \tag{7}$$

is the frame-indifferent Oldroyd derivative and C_D is a dimensionless constant that takes on the value of 1.68 based on a calibration with turbulent channel flow data. The standard K-ϵ model is recovered in the limit as $C_D \to 0$. Both the standard and anisotropic K-ϵ models are solved in conjunction with modeled transport equations for the turbulent kinetic energy K and turbulent dissipation rate ϵ given by[13]

$$\frac{\partial K}{\partial t} + \bar{u}\frac{\partial K}{\partial x} + \bar{v}\frac{\partial K}{\partial y} = \mathcal{P} - \epsilon + \frac{\partial}{\partial x}\left[\left(\nu + \frac{\nu_T}{\sigma_K}\right)\frac{\partial K}{\partial x}\right] + \frac{\partial}{\partial y}\left[\left(\nu + \frac{\nu_T}{\sigma_K}\right)\frac{\partial K}{\partial y}\right] \tag{8}$$

$$\frac{\partial \epsilon}{\partial t} + \bar{u}\frac{\partial \epsilon}{\partial x} + \bar{v}\frac{\partial \epsilon}{\partial y} = C_{\epsilon 1}\frac{\epsilon}{K}\mathcal{P} - C_{\epsilon 2}\frac{\epsilon^2}{K} + \frac{\partial}{\partial x}\left[\left(\nu + \frac{\nu_T}{\sigma_\epsilon}\right)\frac{\partial \epsilon}{\partial x}\right] + \frac{\partial}{\partial y}\left[\left(\nu + \frac{\nu_T}{\sigma_\epsilon}\right)\frac{\partial \epsilon}{\partial y}\right] \tag{9}$$

where $\nu_T \equiv C_\mu(K^2/\epsilon)$ is the eddy viscosity,

$$\mathcal{P} = -\tau_{xx}\frac{\partial \bar{u}}{\partial x} - \tau_{xy}\left(\frac{\partial \bar{u}}{\partial y} + \frac{\partial \bar{v}}{\partial x}\right) - \tau_{yy}\frac{\partial \bar{v}}{\partial y}$$

is the turbulence production, and $C_{\epsilon 1}$, $C_{\epsilon 2}$, σ_K, and σ_ϵ are dimensionless constants that are taken to be 1.44, 1.92, 1.0, and 1.3, respectively. The Reynolds averaged equations (1-9) are solved subject to the following boundary conditions: 1) inlet profiles for $\bar{u}$, K, and ϵ are specified five step heights upstream of the step corner ($\bar{u}$ is taken from the experimental data[3] and the corresponding profiles for K and ϵ are computed from the model formulated for channel flow), 2) the law of the wall is used at the upper and the lower walls, and 3) conservative extrapolated outflow conditions are applied 30 step heights downstream of the step corner; these conditions involve the following: the $\bar{v}$ component of the velocity for the cells at the outflow boundary are obtained by extrapolation, the $\bar{u}$ component of the velocity is then computed by the application of mass balance, and the scalar quantities such as pressure, turbulent kinetic energy, and turbulent dissipation are all obtained by extrapolation. It was found that a downstream channel length of about 30 step heights was needed to ensure that the local error for all of the quantities was of the same order as the interior values.

The law of the wall is applied in two forms. In the standard two-layer form of the law of the wall,

$$\bar{u}^+ = \frac{1}{\kappa}\ell n\, y^+ + 5, \qquad \frac{K}{u_\tau^2} = C_\mu^{-1/2}, \qquad \epsilon = C_\mu^{3/4}\frac{K^{3/2}}{\kappa y} \tag{10}$$

at the first grid point y away from the wall if $y^+ \equiv y u_\tau/\nu \geq 11.6$ given that $\bar{u}^+ \equiv \bar{u}/u_\tau$ (u_τ is the friction velocity and $\kappa = 0.41$ is the von Kármán constant); if $y^+ < 11.6$, then $\bar{u}$, K, and ϵ are interpolated to their wall values based on viscous sublayer constraints.[14] A three-layer law of the wall where

$$\bar{u}^+ = \begin{cases} y^+, & \text{for } y^+ \leq 5 \\ -3.05 + 5\,\ell n\, y^+, & \text{for } 5 < y^+ \leq 30 \\ 5.5 + (1/\kappa)\,\ell n\, y^+, & \text{for } y^+ > 30 \end{cases} \tag{11}$$

is also implemented along the lines of Avva et al.,[12] wherein the fact that the normal derivative of K vanishes at the wall is made use of along with more elaborate interpolation formulas for K and ϵ (see also Ref. 14 for a detailed discussion). The law of the wall does not formally apply to separated turbulent boundary layers. However, since the separation point is fixed at the corner of the back step, and the flowfield is solved iteratively so that the friction velocity u_τ can be updated until it converges, major errors do not appear to result from its use as will be demonstrated in the next section.

The governing equations (1-9) are solved using a finite volume method (see Refs. 15 and 16). Here we are interested in the steady-state solution, which is obtained by solving the

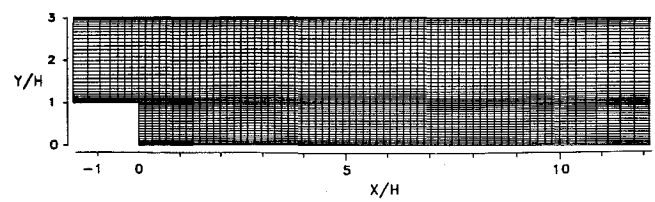

Fig. 2 Computational grid: $E = 1{:}3$; $Re = 1.32 \times 10^5$; 200×100 mesh.

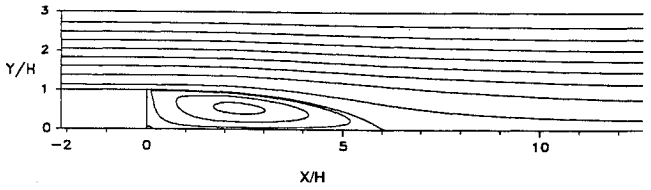

a) Contours of mean streamlines based on two-layer wall model

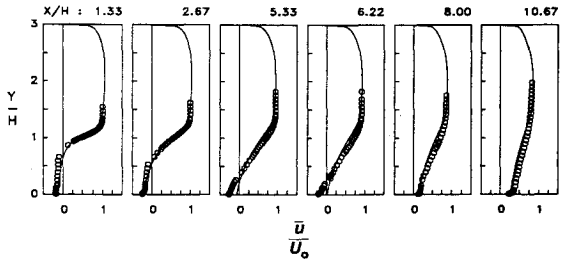

b) Mean velocity profiles at selected locations (—computed solutions based on two-layer wall model; ◦ experiments of Refs. 2 and 3)

Fig. 3 Computed flowfield with the standard K-ϵ model: $E = 1{:}3$; $Re = 1.32 \times 10^5$; 200×100 mesh; $C_\mu = 0.09$; $C_{\epsilon 1} = 1.44$; $C_{\epsilon 2} = 1.92$; $\sigma_K = 1.0$; $\sigma_\epsilon = 1.3$; $\kappa = 0.41$.

system of algebraic equations by a line relaxation method[15] with the repeated application of the tridiagonal matrix solution algorithm.[17] The issue of resolution is crucial for the back-step problem. As discussed by Avva et al.,[12] several researchers have reported results that were in severe error due to a lack of adequate resolution. Thangam and Hur[16] conducted a careful grid refinement study based on this finite volume method for grids containing 166×73 to 332×146 mesh points (these meshes have variable grid spacing to allow for maximum resolution near the step corner and the walls). The conclusion of their study was that a 166×73 mesh yielded results that were within acceptable limits; the use of significantly coarser meshes could lead to appreciable errors. Additional calculations were performed by the same authors that indicate that a 200×100 mesh yields a fully grid independent solution. All of the computations conducted in this study were performed using this 200×100 nonuniform mesh. The computational mesh is illustrated in Fig. 2 (for clarity, only every alternate mesh point is shown for the crucial region $-1 \le X/H \le 12$, which constitutes approximately half of the flow domain). As indicated earlier, the inlet conditions were specified five step heights upstream of the step corner and the outlet boundary conditions were specified 30 step heights downstream of the step corner. It is crucial that a sufficient distance downstream of the reattachment point be allowed before the outflow conditions are imposed. Many earlier computations of the back-step problem were in significant error due to the imposition of fully developed outflow conditions too close to the reattachment point. Furthermore, it is crucial that a fine mesh be used near the step corner for computational accuracy.

The steady-state solution of Eqs. (1-9) is obtained by an iterative solution of the discretized equations. The computed solution was assumed to have converged to its steady state when the root mean square of the average difference between successive iterations was less than 10^{-4} for the mass source.[15,16] Approximately 2000 iterations were needed for the convergence of the standard K-ϵ model; this corresponds to approximately 30 min of CPU time in a partially vectorized mode on the CRAY-2S supercomputer using 64-bit precision. The anisotropic K-ϵ model requires approximately 30% more CPU time due to the fact that the additional correction terms to the standard K-ϵ model have to be evaluated during each iteration. These correction terms are dispersive rather than dissipative—an additional feature that slows convergence.

III. Discussion of the Results

First, results will be presented for the standard K-ϵ model using the two-layer law-of-the-wall boundary conditions. For this case, as well as the others to follow, computed results for the mean velocity streamlines, the streamwise mean velocity profiles, the streamwise turbulence intensity profiles, and the turbulence shear stress profiles are compared with the Kim et al.[2] experimental data as updated by Eaton and Johnston.[3] In Fig. 3a the computed streamlines are shown, indicating reattachment at $X_r/H \approx 6.0$—a result that is approximately a 15% underprediction of the experimental reattachment point of $X_r/H \approx 7.1$. This is in contrast to earlier reported results that seem to indicate that the standard K-ϵ model underpredicts the reattachment point by 20–25%—an exaggerated underprediction due to the lack of adequate resolution in those computations. (A spurious underprediction of the reattachment point can also result from the application of outflow boundary conditions at a distance $X/H < 25$ from the step corner as some authors have done.) In Fig. 3b, the streamwise mean velocity profiles predicted by the standard K-ϵ model are compared with the experimental data. Except in the vicinity of the reattachment point, the comparisons are fairly good. More serious discrepancies between the model predictions and the experimental data occur in the initial part of the recovery zone for the streamwise turbulence intensity profiles, as shown in Fig. 4a. However, the model predictions for the turbulence shear stress profiles are reasonably good, as can be seen from Fig. 4b.

Next, we will examine the effect of the near-wall modeling. In Figs. 5a and 5b, the mean flow streamlines and streamwise mean velocity profiles obtained from the standard K-ϵ model with the three-layer law-of-the-wall boundary condition are shown. With this more accurate version of the law of the wall, the standard K-ϵ model predicts reattachment at $X_r/H \approx 6.25$—a result that is extremely close to that reported by Avva et al.[12] However, the three-layer law of the wall boundary condition does not affect the turbulence stress profiles

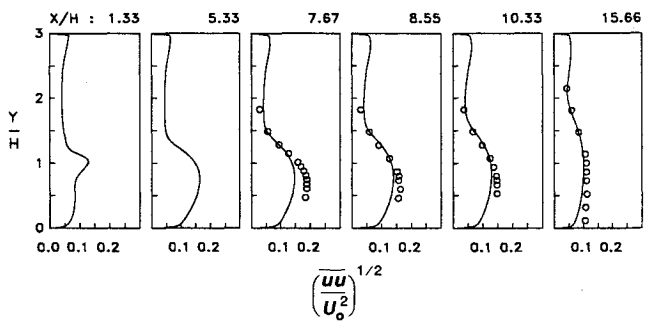

a) Turbulence intensity profiles

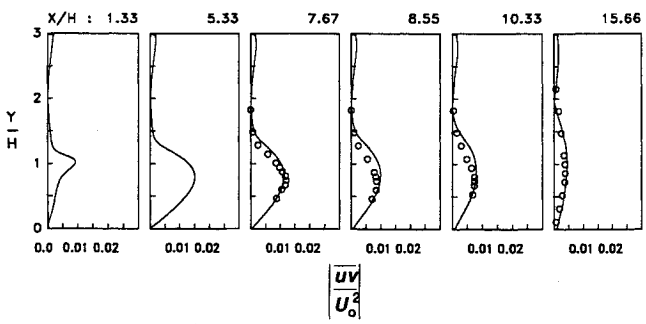

b) Turbulence shear stress profiles

Fig. 4 Computed turbulence stresses with the standard K-ϵ model: $E = 1{:}3$; $Re = 1.32 \times 10^5$; 200×100 mesh; $C_\mu = 0.09$; $C_{\epsilon 1} = 1.44$; $C_{\epsilon 2} = 1.92$; $\sigma_K = 1.0$; $\sigma_\epsilon = 1.3$; $\kappa = 0.41$; —computed solutions based on two-layer wall model; ◦ experiments of Refs. 2 and 3.

appreciably, as illustrated in Figs. 6a and 6b. By integrating the K-ϵ model directly to the wall, with an asymptotically consistent low Reynolds number correction (cf., Refs. 10 and 18), it is possible to improve the prediction for the reattachment point by approximately 5%. Some earlier published work claiming that the near-wall modeling could make a larger difference was in all likelihood due to inadequate resolution of the computations (e.g., Ref. 10 used a 93×66 mesh). Considering the current state of development of near-wall modeling, as well as the relatively small benefits that it can yield for the back-step problem, the remaining results to be shown will be based on the three-layer law-of-the-wall boundary condition. However, for turbulent flows where the separation point is not fixed, near-wall turbulence modeling can play a much more important role.[1]

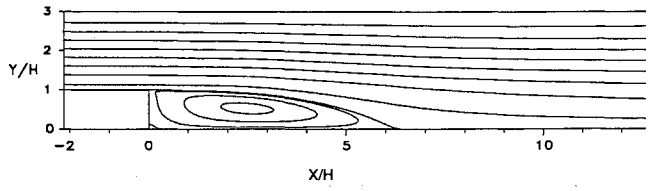

a) Contours of mean streamlines based on three-layer wall model

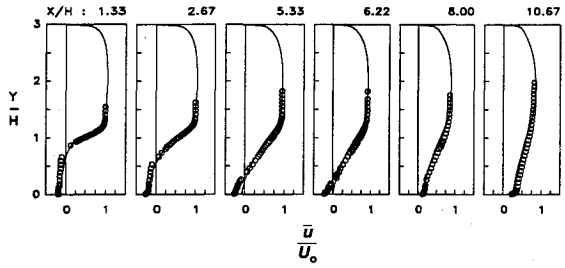

b) Mean velocity profiles at selected locations (—computed solutions based on three-layer wall model; ◦ experiments of Refs. 2 and 3).

Fig. 5 Computed flowfield with the standard K-ϵ model: $E = 1{:}3$; $Re = 1.32 \times 10^5$; 200×100 mesh; $C_\mu = 0.09$; $C_{\epsilon 1} = 1.44$; $C_{\epsilon 2} = 1.92$; $\sigma_K = 1.0$; $\sigma_\epsilon = 1.3$; $\kappa = 0.41$.

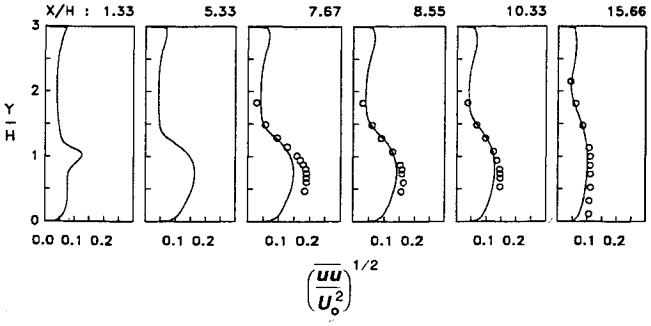

a) Turbulence intensity profiles

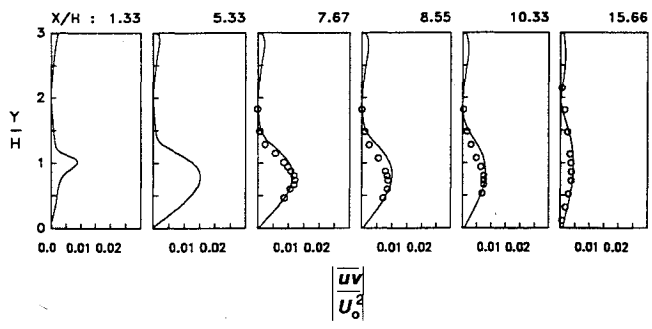

b) Turbulence shear stress profiles

Fig. 6 Computed turbulence stresses with the standard K-ϵ model: $E = 1{:}3$; $Re = 1.32 \times 10^5$; 200×100 mesh; $C_\mu = 0.09$; $C_{\epsilon 1} = 1.44$; $C_{\epsilon 2} = 1.92$; $\sigma_K = 1.0$; $\sigma_\epsilon = 1.3$; $\kappa = 0.41$; —computed solutions based on three-layer wall model; ◦ experiments of Refs. 2 and 3.

Now, it will be demonstrated that the use of the anisotropic eddy-viscosity model (6) can yield a more significant improvement in the results. The computed mean velocity streamlines obtained from the nonlinear K-ϵ model are shown in Fig. 7a. They indicate reattachment at $X_r/H \approx 6.9$: a result that is within 3% of the mean experimental value of $X_r/H \approx 7.1$. Some of the earlier reported results with the nonlinear K-ϵ model (see Refs. 8 and 19) were lower due to insufficient numerical resolution of the flowfield. Surprisingly, despite the fact that the reattachment point is better predicted, there is a slight increase in the deviation of the model predictions from the experimental data for the mean velocity profiles in the separation and recovery zones (see Fig. 7b). This minor anomaly could be due to the dispersive nature of the Oldroyd-derivative terms [see Eq. (7)]. The corresponding streamwise turbulence intensity profiles and turbulence shear-stress profiles are compared with the experimental data in Figs. 8a and 8b. On balance, the agreement between the model predictions and experimental data is acceptable (the uncertainty in the turbulence Reynolds stress measurements is on the order of 10%). The most notable difference between the predictions of the anisotropic and the standard K-ϵ model model lies in the streamwise turbulence intensity located approximately one step height above the corner of the step. Unlike the standard K-ϵ model, the nonlinear K-ϵ model predicts a dramatic trough in this region—a result that is consistent with more recent independent experiments.[20,21] In fact, it is the more accurate prediction of the normal Reynolds stress difference $\tau_{yy} - \tau_{xx}$ that probably accounts for the better predictions of the nonlinear K-ϵ model. The better prediction of normal Reynolds stress differences with an anisotropic eddy viscosity can be illustrated directly in turbulent channel flow. In Fig. 9, the normal Reynolds stress difference predicted by the nonlinear K-ϵ model model is compared with the experimental data of Laufer.[22] It is clear that the nonlinear K-ϵ model does a reasonably good job of reproducing the experimental data, whereas the standard K-ϵ model erroneously predicts that $\tau_{yy} - \tau_{xx} = 0$ (also see Ref. 23). The accurate prediction of this normal Reynolds stress difference is important in the back-

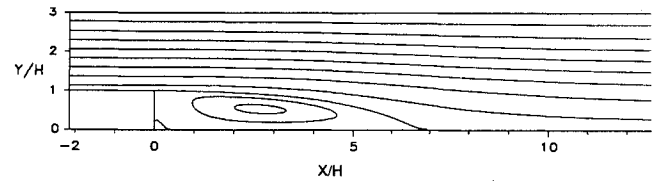

a) Contours of mean streamlines

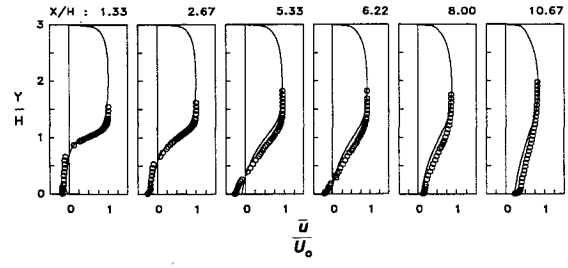

b) Mean velocity profiles at selected locations (—computed solutions based on three-layer wall model; ◦ experiments of Refs. 2 and 3)

Fig. 7 Computed flowfield with the nonlinear K-ϵ model: $E = 1{:}3$; $Re = 1.32 \times 10^5$; 200×100 mesh; $C_\mu = 0.09$; $C_{\epsilon 1} = 1.44$; $C_{\epsilon 2} = 1.92$; $\sigma_K = 1.0$; $\sigma_\epsilon = 1.3$; $\kappa = 0.41$; $C_D = 1.68$.

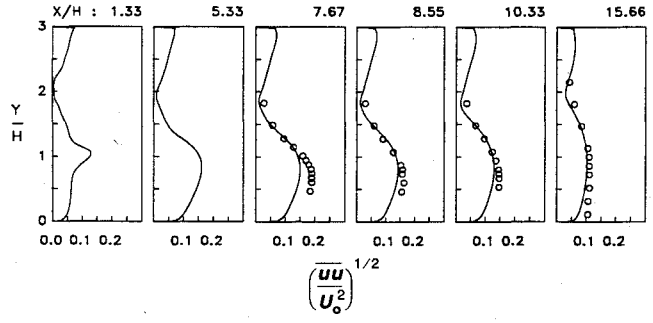

a) Turbulence intensity profiles

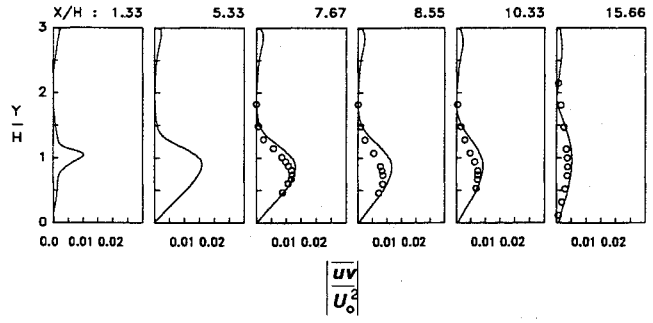

b) Turbulence shear stress profiles

Fig. 8 Computed turbulence stresses with the nonlinear K-ϵ model: $E = 1{:}3$; $Re = 1.32 \times 10^5$; 200×100 mesh; $C_\mu = 0.09$; $C_{\epsilon 1} = 1.44$; $C_{\epsilon 2} = 1.92$; $\sigma_K = 1.0$; $\sigma_\epsilon = 1.3$; $\kappa = 0.41$; $C_D = 1.68$; —computed solutions based on three-layer wall model; ◦ experiments of Refs. 2 and 3.

step problem since the mean flow stream function $\bar{\Psi}$ (where $\bar{u} \equiv -\partial\bar{\Psi}/\partial y$ and $\bar{v} \equiv \partial\bar{\Psi}/\partial x$) is a solution of the transport equation[19]

$$\bar{u}\frac{\partial}{\partial x}(\nabla^2\bar{\Psi}) + \bar{v}\frac{\partial}{\partial y}(\nabla^2\bar{\Psi}) = \nu\nabla^4\bar{\Psi} - \frac{\partial^2(\tau_{yy} - \tau_{xx})}{\partial x \partial y} - \frac{\partial^2\tau_{xy}}{\partial x^2} + \frac{\partial^2\tau_{xy}}{\partial y^2} \tag{12}$$

and, hence, the normal Reynolds stress difference $\tau_{yy} - \tau_{xx}$ contributes directly to the calculation of the mean velocity field. This is the case for any flow with streamline curvature since the normal Reynolds stress term on the right-hand side of Eq. (12) can be converted to the alternate form

$$\frac{\partial^2(\tau_{nn} - \tau_{ss})}{\partial n \partial s}$$

in terms of an intrinsic coordinate system where n and s are, respectively, the normal and tangential directions along a streamline.

The wall pressure coefficient is an important parameter for engineering applications. In Figs. 10a and 10b, the pressure coefficients $C_p[=2(p - p_r)/U_r^2$, where p_r and U_r are the reference pressure and velocity that are taken at the centerline of the inlet] obtained from the standard and nonlinear K-ϵ models at the top and bottom walls are compared with the experimental data of Eaton and Johnston.[3] Both the standard and the nonlinear K-ϵ models perform comparably well in reproducing the experimental trends. In Fig. 10c, the skin-friction coefficients $C_f = 2u_\tau^2/U_r^2$ obtained from the standard and nonlinear K-ϵ models are compared with the scaled experimental data of Driver and Seegmiller[24] for the bottom wall. Here, we make use of the fact that $C_f/C_{f\infty}$, when taken as a function of the normalized distance $(X - X_r)/X_r$, is independent of the expansion ratio given that $C_{f\infty}$ is the fully developed skin-friction coefficient and X_r is the reattachment point. From Fig. 10c it appears that the nonlinear K-ϵ model performs the best; however, both models are well within the uncertainty of the experimental data.

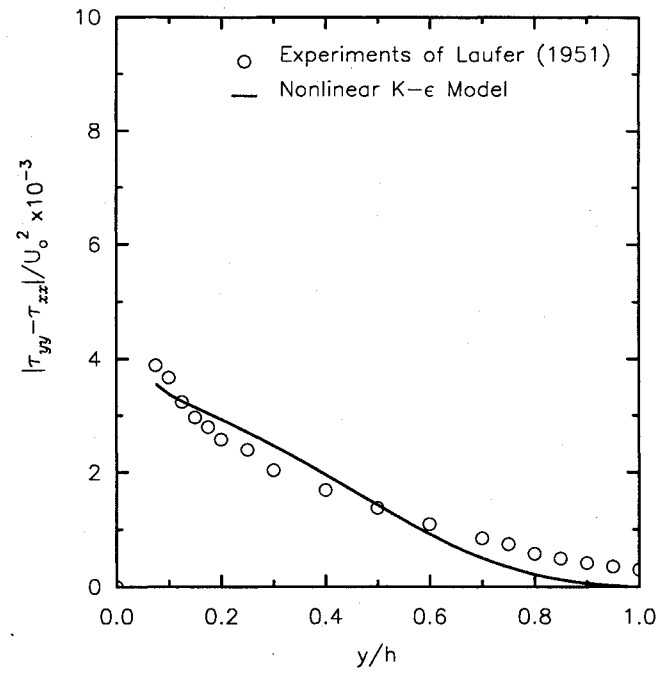

Fig. 9 Comparison of the computed values of the normal Reynolds stress difference obtained from the nonlinear K-ϵ model with the experimental data of Laufer[22] for fully developed turbulent channel flow. (It should be noted that the standard K-ϵ model predicts a zero normal Reynolds stress difference.)

Finally, we will examine the RNG-based K-ϵ model of Yakhot and Orszag.[25] For high-turbulence Reynolds numbers, it is of the same general form as the standard K-ϵ model given by Eqs. (4), (8), and (9). However, the numerical values of the constants, which are computed by the RNG approach, take on the alternate values:

$$C_\mu = 0.0837, \quad C_{\epsilon 1} = 1.063, \quad C_{\epsilon 2} = 1.7215$$
$$\sigma_K = 0.7179, \quad \sigma_\epsilon = 0.7179, \quad \kappa = 0.372$$

For the low-turbulence Reynolds numbers that occur close to the walls in this back-step problem, the RNG K-ϵ model has a built-in correction that allows for a direct integration to a solid boundary with the no-slip condition applied. However, we found this near-wall correction to be rather ambiguous, especially in the presence of geometrical discontinuities such as those that occur near the back-step corners. Hence, we will present results in which we match to the three-layer law of the wall. In Figs. 11a and 11b, the mean flow streamlines and the streamwise mean velocity profiles obtained from the RNG K-ϵ model are shown. The RNG K-ϵ model predicts reattachment at $X_r/H \approx 4$—a result that constitutes a substantial underprediction of the experimental reattachment point of $X_r/H \approx 7.1$. Because of this significant underprediction of the reattachment point, the streamwise turbulence intensity and turbulence shear-stress profiles predicted by the RNG K-ϵ model are in serious error, as illustrated in Figs. 12a and 12b. The origin of this substantial underprediction of the reattachment point lies in the choice of $C_{\epsilon 1} = 1.063$. In a homogeneous shear flow, it can be shown that the eddy viscosity

$$\nu_T \sim \exp(\lambda t^*) \tag{13}$$

where t^* is the time (nondimensionalized by the shear rate) and λ is the growth rate given by[26]

$$\lambda = \left[\frac{C_\mu(C_{\epsilon 2} - C_{\epsilon 1})^2}{(C_{\epsilon 1} - 1)(C_{\epsilon 2} - 1)}\right]^{1/2} \tag{14}$$

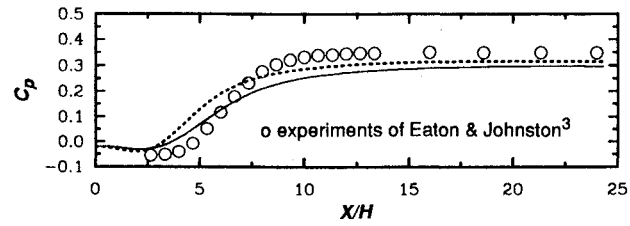

a) Pressure coefficient along the bottom wall (◦ experiments of Ref. 3)

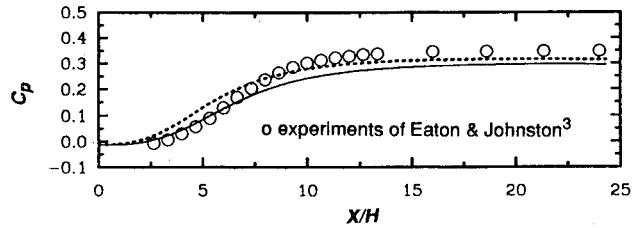

b) Pressure coefficient along the top wall (◦ experiments of Ref. 3)

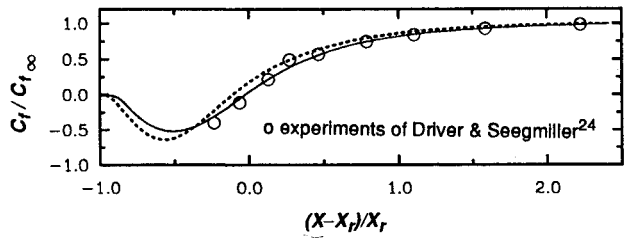

c) Skin-friction coefficient along the bottom wall (◦ scaled experimental data of Ref. 24)

Fig. 10 Comparison of the predicted wall distributions with experiments: --- standard K-ϵ model; —nonlinear K-ϵ model.

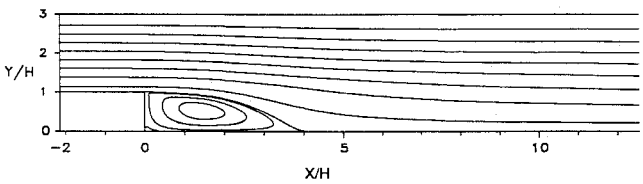

a) Contours of mean streamlines

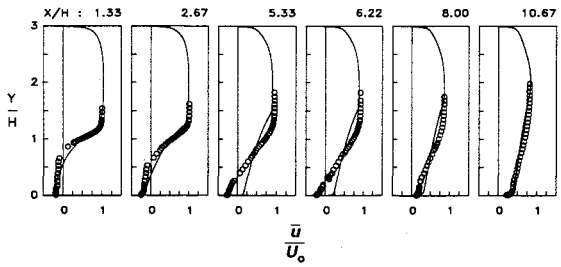

b) Mean velocity profiles at selected locations (—computed solutions based on three-layer wall model; ◦ experiments of Refs. 2 and 3).

Fig. 11 Computed flowfield with the RNG K-ϵ model: E = 1:3; $Re = 1.32 \times 10^5$; 200×100 mesh; $C_\mu = 0.0837$; $C_{\epsilon 1} = 1.063$; $C_{\epsilon 2} = 1.7215$; $\sigma_K = \sigma_\epsilon = 0.7179$; $\kappa = 0.372$.

Hence, the growth rate of the eddy viscosity becomes singular as $C_{\epsilon 1} \to 1$. For $C_{\epsilon 1} = 1.063$, as opposed to the more standard value of $C_{\epsilon 1} = 1.44$, the growth rate of the eddy viscosity will be overly large. An overprediction of the eddy viscosity in shear flows will make the model too dissipative—a feature that will cause the separation bubble to shorten, as shown in Fig. 11a. Hence, whereas the use of an alternate near-wall treatment with the RNG K-ϵ model could cause the separation bubble to become slightly larger, we think that it is very unlikely that a reattachment point close to $X_r/H \approx 7$ could be obtained using this RNG K-ϵ model as reported in Karniadakis et al.[11] It should be noted, however, that Yakhot and Smith[27] have recently determined that there was an error in the original calculation of $C_{\epsilon 1}$ by Yakhot and Orszag[25]; they obtained an alternate value of $C_{\epsilon 1} = 1.42$. With this higher value of $C_{\epsilon 1}$, and with the use of an RNG-based anisotropic eddy viscosity (see Ref. 28), it is likely that the RNG K-ϵ model would yield good results for the back-step problem.

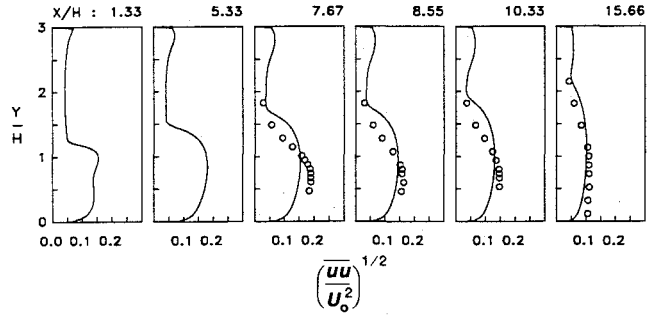

a) Turbulence intensity profiles

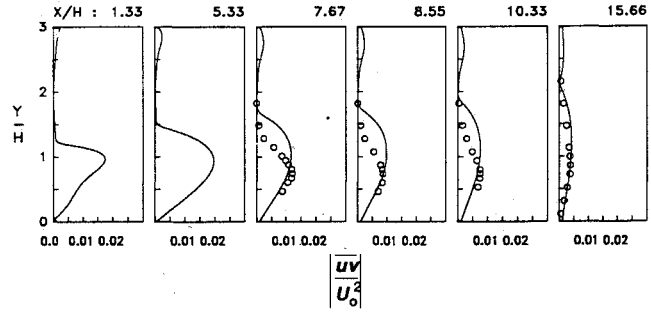

b) Turbulence shear stress profiles

Fig. 12 Computed turbulence stresses with the RNG K-ϵ model: E = 1:3; $Re = 1.32 \times 10^5$; 200×100 mesh; $C_\mu = 0.0837$; $C_{\epsilon 1} = 1.063$; $C_{\epsilon 2} = 1.7215$; $\sigma_K = \sigma_\epsilon = 0.7179$; $\kappa = 0.372$; —computed solutions based on three-layer wall model; ◦ experiments of Refs. 2 and 3.

IV. Conclusions

A theoretical and computational analysis of the performance of two-equation turbulence models for turbulent flow past a backward-facing step has been presented in an effort to resolve numerous conflicting studies that have been published during the past 10 years. The following general conclusions were obtained.

1) The standard K-ϵ model with three-layer wall functions predicts reattachment at $X_r/H \approx 6.25$—a result that is within 12% of the experimental value of Kim et al.[2] for the back-step problem considered here. This result is in close agreement with the recent computations of Avva et al.[12] and, hence, there is little doubt that earlier studies that attributed a 20–25% underprediction of the reattachment point to the standard K-ϵ model were in error due to inadequate numerical resolution of the flowfield.

2) When the standard K-ϵ model is appropriately modified to include an anisotropic eddy viscosity,[8] the reattachment point moves out to $X_r/H \approx 6.9$. This result, as well as the other mean velocity statistics, are within 3% of the experimental data—an improvement due to the more accurate prediction of normal Reynolds stress differences.

3) The RNG K-ϵ model of Yakhot and Orszag[25] substan-

tially underpredicts the reattachment point. This problem arises since $C_{\epsilon 1}$ is too close to 1—a feature that causes the model to be overly dissipative (e.g., when $C_{\epsilon 1} = 1$, the growth rate of the eddy viscosity becomes singular in homogeneous shear flow). However, it is likely that with the recent suggested correction of $C_{\epsilon 1}$ to 1.42,[27] and with the use of an anisotropic eddy viscosity, the RNG K-ϵ model would yield good results for the back-step problem.

Finally, some remarks are in order concerning the implications that these results have for turbulence modeling. The deficiencies of two-equation models are well established, particularly in turbulent flows with body forces or Reynolds stress relaxation effects.[26] Consequently, the findings of this study should not be interpreted as an unequivocal endorsement of two-equation models. Nonetheless, this study certainly does indicate that properly calibrated two-equation turbulence models, with an anisotropic eddy viscosity, can yield results for the back-step problem that are far superior to the results obtained from the older zero- or one-equation models.

Acknowledgment

This research was supported by NASA under Contract NAS1-18605 while the authors were in residence at the Institute for Computer Applications in Science and Engineering, NASA Langley Research Center, Hampton, VA 23665.

References

[1]Kline, S. J., Cantwell, B. J., and Lilley, G. M. (eds.), *Proceedings of the 1980-81 AFOSR-HTTM Stanford Conference on Complex Turbulent Flows,* Stanford Univ. Press, Stanford, CA, 1981.

[2]Kim, J., Kline, S. J., and Johnston, J. P., "Investigation of a Reattaching Turbulent Shear Layer: Flow Over a Backward-Facing Step," *Journal of Fluids Engineering,* Vol. 102, No. 3, 1980, pp. 302–308.

[3]Eaton, J., and Johnston, J. P., "Turbulent Flow Reattachment: An Experimental Study of the Flow and Structure Behind a Backward-Facing Step," Stanford Univ., TR MD-39, Stanford, CA, June 1980.

[4]Sindir, M. M. S., "Effects of Expansion Ratio on the Calculation of Parallel-Walled Backward-Facing Step Flows: Comparison of Four Models of Turbulence," Ph.D. Dissertation, Univ. of California, Davis, CA, 1982.

[5]Gibson, M. M., "An Algebraic Stress and Heat Flux Model for Turbulent Shear Flow with Streamline Curvature," *International Journal of Heat and Mass Transfer,* Vol. 21, No. 12, 1978, pp. 1609–1617.

[6]Chen, C. P., "Multiple Scale Turbulence Closure Modeling of Confined Recirculating Flows," NASA CR-178536, Aug. 1985.

[7]Hanjalic, K., Launder, B. E., and Schiestel, R., "Multiple-Time Scale Concepts in Turbulent Shear Flows," *Turbulent Shear Flows,* edited by L. J. S. Bradbury, F. Durst, B. E. Launder, F. W. Schmidt, and J. H. Whitelaw, Vol. 2, Springer-Verlag, New York, 1980, pp. 36–49.

[8]Speziale, C. G., "On Nonlinear K-l and K-ϵ Models of Turbulence," *Journal of Fluid Mechanics,* Vol. 178, 1987, pp. 459–475.

[9]Benocci, C., and Skovgaard, M., "Prediction of Turbulent Flow Over a Backward-Facing Step," *Numerical Methods for Laminar and Turbulent Flows,* edited by C. Taylor, P. Gresho, R. L. Sani, and J. Haüser, Vol. 6, Pineridge, UK, 1989, pp. 655–665.

[10]So, R. M. C., Lai, Y. G., Hwang, B. C., and Yao, G. J., "Low-Reynolds-Number Modeling of Flows Over a Backward-Facing Step," *ZAMP,* Vol. 39, No. 1, 1988, pp. 13–27.

[11]Karniadakis, G., Yakhot, A., Rakib, S., Orszag, S. A., and Yakhot, V., "Spectral Element—RNG Simulations of Turbulent Flows in Complex Geometries," *Proceedings of the Seventh Symposium on Turbulent Shear Flows,* edited by F. Durst, B. E. Launder, F. W. Schmidt, and J. H. Whitelaw, Stanford Univ. Press, Stanford, CA, 1989; paper 7.2.

[12]Avva, R. K., Kline, S. J., and Ferziger, J. H., "Computation of the Turbulent Flow Over a Backward-Facing Step Using the Zonal Modeling Approach," Stanford Univ., TR TF-33, Stanford, CA, 1988; also AIAA Paper 88-0611, Jan. 1988.

[13]Launder, B. E., and Spalding, D. B., "The Numerical Computation of Turbulent Flows," *Computer Methods in Applied Mechanics & Engineering,* Vol. 3, 1974, pp. 269–289.

[14]Amano, R. S., "Development of a Turbulent Near-Wall Model and Its Application to Separated and Reattached Flows," *Numerical Heat Transfer,* Vol. 7, 1984, pp. 59–75.

[15]Lilley, D. G., and Rhode, D. L., "A Computer Code for Swirling Turbulent Axisymmetric Recirculating Flows in Practical Isothermal Combustor Geometries," NASA CR-3442, Feb. 1982.

[16]Thangam, S., and Hur, N., "A Highly Resolved Numerical Study of Turbulent Separated Flow Past a Backward-Facing Step," *International Journal of Engineering Science,* Vol. 29, No. 5, 1991, pp. 607–615.

[17]Isaacson, E., and Keller, H. B., *Analysis of Numerical Methods,* Wiley, New York, 1970.

[18]Speziale, C. G., Abid, R., and Anderson, E. C., "A Critical Evaluation of Two-Equation Models for Near-Wall Turbulence," AIAA Paper 90-1481, June 1990.

[19]Speziale, C. G., and Ngo, T., "Numerical Solution of Turbulent Flow Past a Backward-Facing Step Using a Nonlinear K-ϵ Model," *International Journal of Engineering Science,* Vol. 26, No. 10, 1988, pp. 1099–1112.

[20]Meyers, J. F., Kjelgaard, S. O., and Hepner, T. E., "Investigation of Particle Sampling Bias in a Shear Flow Field Downstream of a Backward Facing Step," *Fifth International Symposium on Applications of Laser Technologies to Fluid Mechanics,* Lisbon, Portugal, July 1990.

[21]Thangam, S., Kjelgaard, S. O., and Speziale, C. G., "Investigation of Turbulent Flow Past a Backward-Facing Step: Modeling and Experiments," *Bulletin of the American Physical Society,* Vol. 35, No. 10, 1990, p. 2324.

[22]Laufer, J., "Investigation of Turbulent Flow in a Two-Dimensional Channel," NACA TN 1053, 1951.

[23]Hur, N., Thangam, S., and Speziale, C. G., "Numerical Study of Turbulent Secondary Flows in Curved Ducts," *Journal of Fluids Engineering,* Vol. 112, No. 2, 1990, pp. 205–211.

[24]Driver, D. M., and Seegmiller, H. L., "Features of a Reattaching Turbulent Shear Layer in Divergent Channel Flow," *AIAA Journal,* Vol. 23, No. 2, 1985, pp. 163–171.

[25]Yakhot, V., and Orszag, S. A., "Renormalization Group Analysis of Turbulence. I. Basic Theory," *Journal of Scientific Computing,* Vol. 1, No. 1, 1986, pp. 3–51.

[26]Speziale, C. G., "Analytical Methods for the Development of Reynolds Stress Closures in Turbulence," *Annual Review of Fluid Mechanics,* Vol. 23, 1991, pp. 107–157.

[27]Yakhot, V., and Smith, L., "The Renormalization Group, the ϵ-expansion and Derivation of Turbulence Models," *Journal of Scientific Computing* (to be published).

[28]Rubinstein, R., and Barton, J. M., "Nonlinear Reynolds Stress Models and the Renormalization Group," *Physics of Fluids A,* Vol. 2, No. 8, 1990, pp. 1472–1476.